THE UNIVERSITY OF NOTTINGHAM

SIR PETER MANSFIELD IMAGING CENTRE

SCHOOL OF PHYSICS AND ASTRONOMY

Developing Techniques for Quantitative Renal Magnetic Resonance Imaging

Author:
Alexander James DANIEL MSci

Supervisor:
Prof. Susan FRANCIS

15th February, 2021

Thesis submitted to the University of Nottingham for the degree of Doctor of Philosophy

It's very hard to talk quantum using a language originally designed to tell other monkeys where the ripe fruit is.

Terry Pratchett, *Night Watch*

Abstract

Science will happen, but this bit can be read by muggles on 'tinterweb.

Contents

Todo list

Chapter 4

Quantitative Methods to Measure Renal Oxygenation

Abstract

Measurements of oxygenation of blood entering and leaving the kidneys would be a highly desirable quantitative biomarker allowing the calculation of renal metabolic rate of oxygen. Two methods of measuring blood oxygen saturation using MRI have been developed for use in the brain, Susceptibility Based Oximetry (SBO) and T_2 Relaxation Under Spin Tagging (TRUST).

Here both methods are tailored for use in the abdomen, these modified sequences are compared to their unmodified counterparts in the controlled environment of the brain, verifying that the modifications do not affect the quantitative accuracy. The methods are then applied to measure oxygenation in the renal vein. The geometry of the renal vessels leads to a high degree of uncertainty when applying SBO however TRUST produced results concordant with literature.

To verify the TRUST was able to measure a change in renal oxygenation, a hyperoxia challenge was undertaken. Measurements of oxygen saturation in the renal vein were collected using TRUST and BOLD T_2^* maps, the current standard for assessing renal oxygenation, were collected while the subject was breathing room air, then pure oxygen. A 16 ± 3 % increase in oxygenation was measured using TRUST whereas no significant difference in T_2^* was measured.

This work was presented as an aural presentation at the International Society of Magnetic Resonance in Medicine (ISMRM) 26th Annual Meeting (2018) [1].

4.1 Introduction

As part of a multi-parametric quantitative Magnetic Resonance Imaging (MRI) protocol, Section 1.2, properties such as haemodynamics, oxygenation, and microstructure are assessed in a single 45 minute scanning session [2, 3]. Currently oxygenation is assessed using Blood Oxygen Level Dependent (BOLD) T_2^* maps to measure oxygenation of different tissues within the kidney, predominately the separation in mean T_2^* between the renal cortex and medulla, an example of which is shown in Figure 4.1. These BOLD T_2^* maps are, however, affected by other factors such as susceptibility effects, shimming and baseline blood flow and thus may be limited in their ability to draw quantitative conclusions despite their widespread use [4, 5].

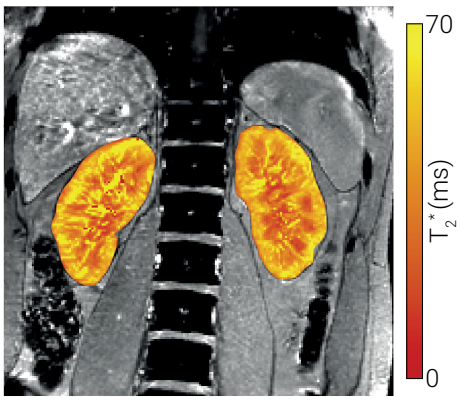

Figure 4.1: An example T_2^* map. A clear difference can be seen between the renal medulla and cortex.

A welcome addition to this multi-parametric model would be the assessment of Renal Metabolic Rate of Oxygen ($RMRO_2$); a measure analogous to the Cerebral Metabolic Rate of Oxygen ($CMRO_2$) [6]. This measure can be calculated via Equation (4.1),

$$RMRO_2 = (Y_a - Y_v) \times RBF \times [Hct] \tag{4.1}$$

where Y_a and Y_v are arterial and venous oxygen saturation respectively, RBF is renal blood flow (in mℓ/min) and Hct is the ratio of the volume of erythro-

cytes to the volume of the rest of the blood, known as haematocrit. RBF can be measured relatively easily using Phase Contrast (PC)-MRI [7] and Hct is usually taken to be 0.41 for healthy adults but can be measured from a simple blood test [8, 9] or using the correlation between T_1 of blood and its haematocrit [10]. This means that only a measurement of blood oxygen saturation via a non-invasive protocol is required to generate a quantitative value of $RMRO_2$.

Blood oxygen saturation can be measured precisely via the insertion of catheters into the subject, however this is clearly an invasive process [11]. There are currently two well established methods of measuring blood oxygenation via MRI however, thus far, these techniques have only been used to measure oxygen saturation in the sagittal sinus, a prominent vein in the brain. These methods are T_2 Relaxation Under Spin Tagging (TRUST) [12–15] and Susceptibility Based Oximetry (SBO) [16–19]. TRUST builds on the ideas of an Arterial Spin Labelling (ASL) sequence in the fact that by subtracting control images from labelled images only blood is imaged. However, instead of labelling a slab of tissue in the neck and imaging a superior slice, when implementing TRUST the imaging plane is inferior to the labelled slab. By collecting a series of pairs of labelled and control images with different T_2 weightings it is possible to fit the data from the sagittal sinus to a T_2 relaxation and use a calibration curve to convert the value of T_2 to venous oxygenation [20]. SBO is based upon the differences in magnetic susceptibility between the blood and the surrounding tissue. Using a phase map it is possible to model this difference in susceptibility and using the known difference in susceptibility between fully oxygenated blood and fully deoxygenated blood, venous oxygenation can be calculated.

Here both of the above techniques are applied to study oxygenation in the renal vein in young healthy individuals to assess the technicalities of transferring these protocols from the brain to the body. Given that these techniques have already been used in the brain with a number of studies in the literature, the sequences are first implemented on the brain to assess oxygenation in the

superior sagittal sinus, then adapted to work within the more challenging environment of applications within the abdomen. These adapted sequences are compared to the results gained using the established techniques in the brain before testing on the renal vein. An oxygen challenge is carried out to verify that changes in oxygenation can be measured in the renal vein. If proved successful these sequences will be incorporated into the multi-parametric renal MRI protocol.

4.2 Methods

Imaging was performed on a whole body 3 Tesla MRI scanner (Ingenia, Philips Medical Systems, The Netherlands) using a 32 channel head or body coil. Studies were carried out according to the principles of the Declaration of Helsinki and approved by either the Local Ethics Committee or the East Midlands Research Ethics Committee. Written informed consent was obtained from all subjects.

4.2.1 Susceptibility-Based Oximetry

MRI Protocol

The principle behind SBO is based on the fact that there is a difference in magnetic susceptibility between the blood within a vessel and the tissue surrounding it [21]. As outlined by Jain, if a blood vessel is modelled as a long paramagnetic cylinder, it is possible to calculate the oxygenation of the blood by knowing the phase difference between blood in the vessel and the surrounding tissue, the angle of the vessel to the B_0 field, the echo time of the scan and the subject's haematocrit [16]. This relationship is given by,

$$\mathrm{Y_v} = \left[1 - \frac{2|\Delta\phi|}{\gamma TE\Delta\chi_{\mathrm{do}}B_0(\cos^2\theta - 1/3)\mathrm{Hct}}\right] \times 100, \tag{4.2}$$

where $\Delta\phi$ is the average phase difference between the blood in the vessel and the surrounding tissue, γ is the gyromagnetic ratio of a proton, TE is the echo time, $\Delta\chi_{\mathrm{do}}$ is the susceptibility difference between fully deoxygenated and fully oxygenated blood ($4\pi \times 0.27$p.p.m) [22, 23], B_0 is the static field strength, θ is the angle of the vessel to the B_0 field and Hct is the subjects haematocrit. Given haematocrit can be assumed or is measured with a blood test or by measuring the T_1 of the blood, this means that from a simple phase map it is possible to calculate Y_v. The optimum phase map for this purpose was produced using a 2D T_1 weighted Fast Field Echo (FFE) sequence with a

flip angle of 25°, flow compensation, coil homogeneity correction and flyback. The Field Of View (FOV) was 230×184×29 mm, matrix size of 400×300, Repetition Time (TR) of 12 ms, Echo Time (TE) of 7.5 ms and three signal averages. This led to a total acquisition time of 9 seconds and as such could be completed in a single breath hold if required.

Analysis

Once the phase map has been acquired, a Region Of Interest (ROI) containing the superior sagittal sinus was defined. This mask was then dilated with concentric shells to generate the two ROI shown in Figure 4.2, note that the outer ROI has been constrained to within the brain during its dilation. There were no occurrences of phase wrapping in or immediately surrounding the superior sagittal sinus observed due to its small size and the high field homogeneity within the head and of the 3T scanner used. Any occurrences of phase wrapping could easily be corrected using Phase Region Expanding Labeller for Unwrapping Discrete Estimates (PRELUDE), a tool within fMRIB Software Library (FSL) (fMRIB, The University of Oxford) [24]. The average values of phase within these two ROI along with the angle of the vessel to the B_0 field, as calculated from the localisation scans can then be used with Equation (4.2) to calculate Y_v.

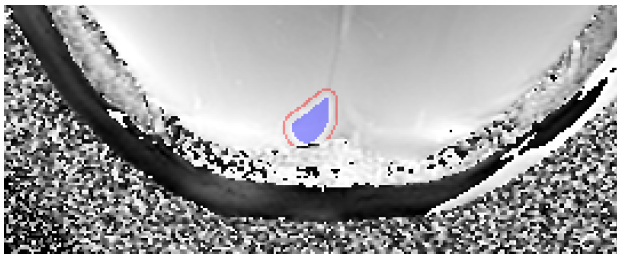

Figure 4.2: The region of interest averaged to find the intra-vascular phase (blue) and the region of interest used to find the phase of the surrounding tissue (red).

4.2.2 T_2 Relaxation Under Spin Tagging

MRI Protocol

The protocol for the TRUST MRI sequence in the brain involves the acquisition of a series of paired images using the pulse sequence shown in Figure 4.3a. A series of presaturation pulses using the Water suppression Enhanced through T_1 effects (WET) scheme are applied to the imaging slice, shown in Figure 4.3b, to reduce the signal from static tissue and reduce contamination of the magnetisation in the imaging slice by an imperfect labelling slab profile [25, 26]. In the first of each image pair, a labelling pulse is applied consisting of two successive slice-selective 90° Radio Frequency (RF) pulses to generate a 180° label. The next image in the sequence has a control pulse applied to it instead of a labelling pulse, in this image the second of the 90° pulses is applied 180° out of phase to give zero net effect. As such any effects of magnetisation transfer related signal in the stationary tissue can be cancelled out because the net RF effect on the macromolecular spin magnetization is identical for both the labelling pulse and control pulse. This method of labelling is known as Transfer Insensitive Labelling Technique (TILT) and is widely used in literature for labelling in TRUST in the brain [27]. A series of non-selective T_2 preparation pulses are then applied to minimise the blood outflow effect and modulate the T_2 weighting of the image as in the Carr-Purcell-Meiboom-Gill (CPMG) sequence in Chapter 3, the time between the application of the labelling pulse and the T_2 preparation is known as the Post Label Delay (PLD). Finally a 90° excitation pulse is applied followed by a standard Echo Planar Imaging (EPI) readout at time TE later [13]. If the control image is subtracted from the labelled image then only the venous blood that flowed from the labelled slab to the imaging slice will be visible, as shown in Figure 4.4.

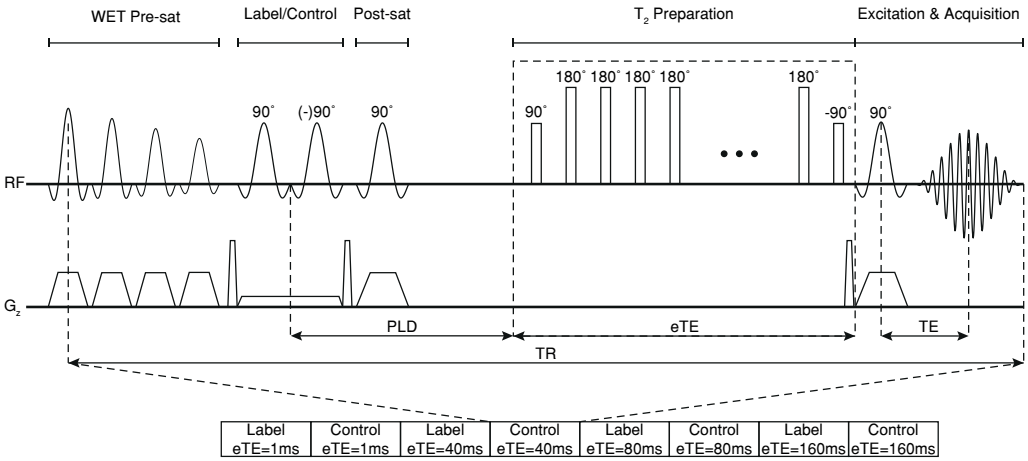

(a)

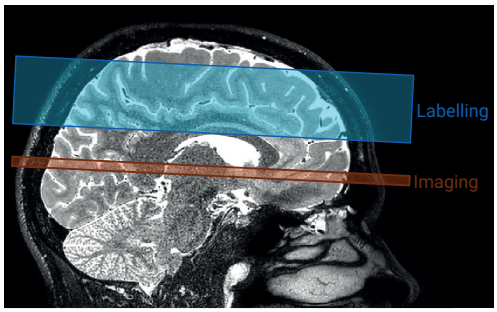

(b)

Figure 4.3: (a) The pulse sequence for TRUST MRI using the TILT labelling sequence. (b) The labelling and imaging volumes used for TILT tagging within the brain.

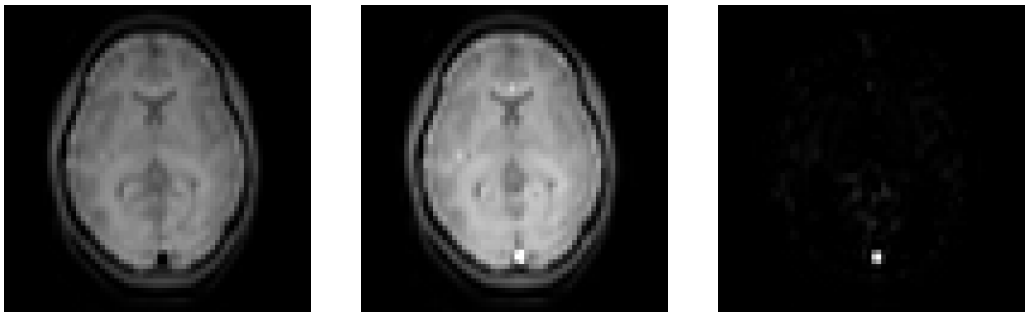

(a) (b) (c)

Figure 4.4: The control image, (a), is subtracted from the labelled image, (b), to generate a difference image, (c), of only the tagged blood.

This process is then repeated for another pair of images, however, this time the duration of the T_2 preparation is increased to a larger Effective Echo Time (eTE), this applies a T_2 weighting to the image in addition to the constant weighting caused by the regular TE. Three label/control image pairs were acquired with each eTE of 1 ms, 40 ms, 80 ms and 160 ms.

The resulting signal in the superior sagittal sinus of the difference between the labelled image and control image, ΔS, is defined by Equation (4.3)

$$\begin{aligned} \Delta S &= S_{\text{label}} - S_{\text{control}} \\ &= S_{\text{blood label}} - S_{\text{blood control}} \\ &= S_0 e^{eTE(1/T_1 - 1/T_2)} \end{aligned} \tag{4.3}$$

where $S_0 = 2e^{-TI/T_1 - TE/T_2^*}$ and; T_1, T_2 and T_2^* are the relaxation constants of blood. If it is assumed that T_1 of blood is approximately 1624 ms [28] then it is possible to fit the collected data to a mono-exponential function and find an estimate of T_2. It is deemed acceptable to use a mean value of T_1 as it will always be much greater than the value of T_2 and thus the possible small changes in T_1 due to blood oxygenation and haematocrit become negligible when fitting the T_2 curve.

The final step in this procedure is to convert the value of T_2 into one of

Y_v. The relationship between T_2 and Y_v is relatively well known and as such a simple empirically derived calibration curve can be used for this conversion, Figure 4.5 [9, 29, 30].

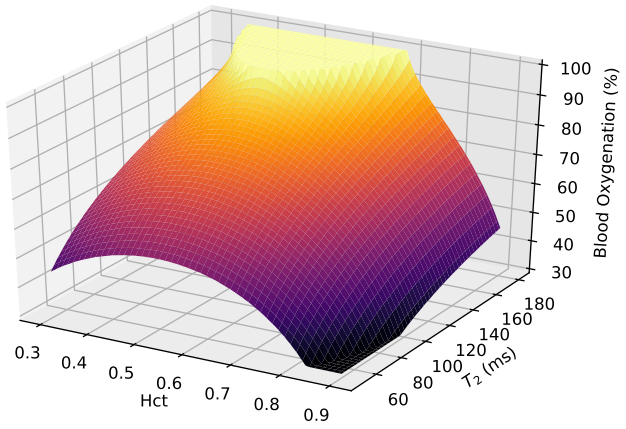

Figure 4.5: The calibration curve used to convert between T_2 and Y_v for a given haematocrit [31].

The parameters used in the brain TILT TRUST sequence were as follows: label slab thickness = 100 mm, imaging slice thickness = 5 mm, distance between centre of imaging slice and centre of labelling slice = 75 mm, FOV = 220×220×5 mm, matrix size = 64×64, voxel size = 3.44 × 3.44 mm, Sensitivity Encoding (SENSE) = 3, EPI factor = 15, T_1 = 1624 ms, PLD = 1022 ms, the choice of this value will be explored later, TR = 3000 ms, TE = 2.9 ms, eTE = 1 ms, 40 ms, 80 ms and 160 ms with three pairs of images acquired at each. This led to a total scan duration of approximately 84 seconds.

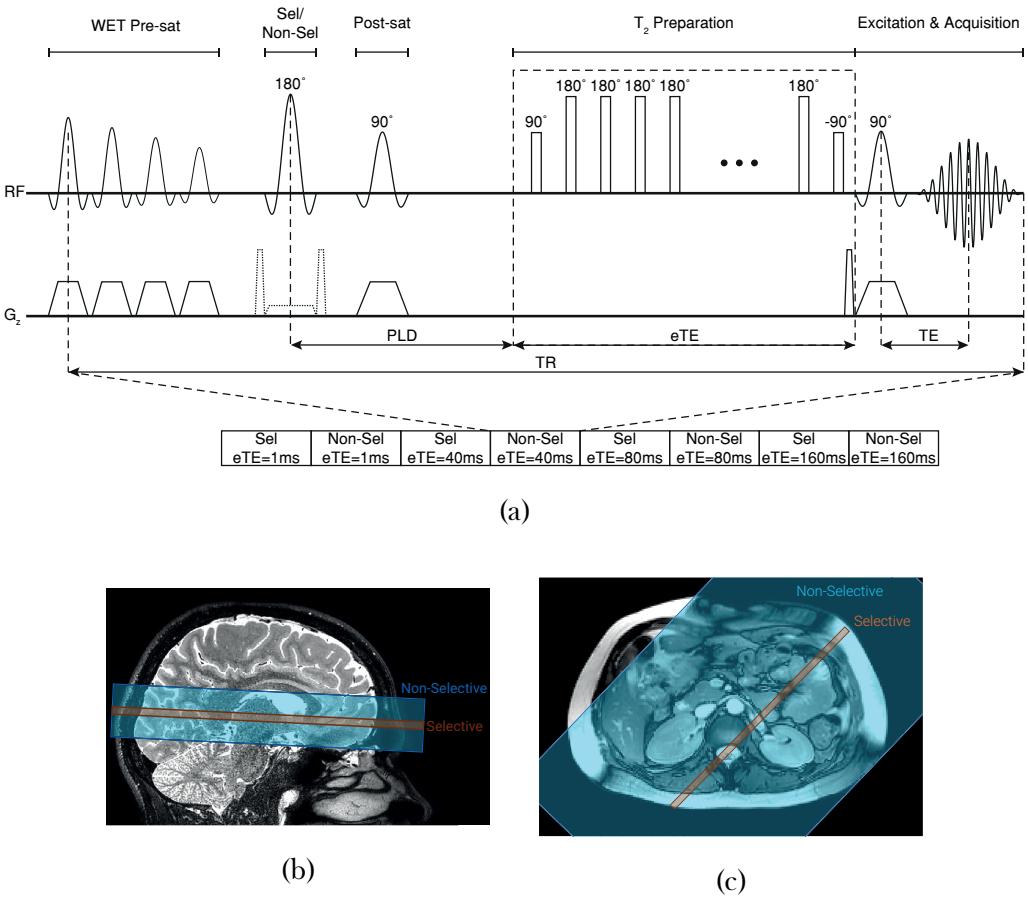

Figure 4.6: (a) The pulse sequence for TRUST MRI using the FAIR labelling sequence. (b) The selective and non-selective volumes used for tagging via FAIR in the brain. (c) The selective and non-selective volumes used for tagging via FAIR in the kidneys.

The main hurdle to be overcome when moving TRUST to the body is the inhomogeneity in the magnetic field caused by the far less homogeneous tissue susceptibilities within the body compared to the brain. These inhomogeneities mean that it is not possible to use TILT as the labelling method, instead the Flow-sensitive Alternating Inversion Recovery (FAIR) labelling scheme will be used [32], a diagram of this pulse sequence is shown in Figure 4.6a. In the FAIR labelling scheme a selective inversion pulse is applied with slice selective gradients turned on followed by T_2 preparation and acquisition to generate the first image in the pair, a non-selective inversion pulse is then applied with a lower slice selective gradient followed by T_2 preparation and then acquisition to generate the second image. An example of the raw

images produced is shown in Figure 4.7. A schematic of the selective and non-selective slices in the brain and the renal vein are shown in Figures 4.6b and 4.6c respectively. This sequence also has the advantage of being far easier to plan. In the brain having a separate labelling and imaging slice is relatively trivial however the flow of blood in the body is far less ordered and as such, the use of a selective slab within a non-selective slab yields far better results. Movement is a much greater problem in the body. Given the long acquisition time of TRUST it is impossible to carry out the scan in a breath hold, as such the sequence is respiratory triggered via a respiratory belt applied around the subjects chest. The total scan time is therefore dependent upon respiratory rate. Depending on the subject, a delay can be applied between the respiratory trigger and the labelling pulse to acquire images while the subject has fully exhaled.

(a) (b) (c)

Figure 4.7: The raw images generated when using the FAIR labelling sequence on the kidneys. The non-selective image, (a), is subtracted from the selective image, (b), and generates (c), an image of only the untagged blood. The raw FAIR images from the brain are omitted as they are very similar to those seen in Figure 4.4.

When using the FAIR labelling sequence on the brain the following parameters were used: selective slab thickness = 25 mm, non-selective slab thickness = 400 mm, FOV = 220×220×5 mm, matrix size = 64×64, voxel size = 3.44 × 3.44 × 5 mm, SENSE = 3, EPI factor = 15, T_1 = 1624 ms, PLD = 800 ms, TR = 7276 ms, TE = 2.9 ms, eTE = 1 ms, 40 ms, 80 ms and 160 ms with three pairs of images acquired at each. When used on the body, the para-

meters were as follows: selective slab thickness = 25 mm, non-selective slab thickness = 400 mm, FOV = 244×244×5 mm, matrix size = 96×96, voxel size = 3.44 × 3.44 × 5 mm, SENSE = 3, EPI factor = 15, T_1 = 1624 ms, PLD = 1000 ms, the choice of this value will be explored later, TR = 8076 ms, TE = 2.9 ms, eTE = 1 ms, 40 ms, 80 ms and 160 ms with three pairs of images acquired at each.

Analysis

The analysis of the data collected using the above protocol was carried out using custom MATLAB (MathWorks, Natick, MA) software based upon code written by Liu and modified to work with data collected using the FAIR labelling method [33]. This software loads the data and carries out the subtraction of each image pair then presents a difference image to the user so the vessel can be drawn around. At this point the voxels with the greatest intensity within the vessel, four voxels when calculating Y_v for the superior sagittal sinus and nine voxels when working on the renal vein, are averaged, as are the intensities of each repeat eTE. These mean signals are then fit to Equation (4.3) to compute a value of T_2 with confidence bounds. The value of Y_v can then be found using the aforementioned calibration curve. Once the software has finished, it saves all outputs and intermediary variables to a file on the computer for later analysis.

4.2.3 Inducing Changes in Oxygenation of Blood in the Renal Vein

In order to assess the ability of these methods to measure a change in renal oxygenation, a method of inducing such a change in the kidneys needed to be devised. Looking at literature that has carried out similar studies, it is suggested that changes in renal oxygenation can be induced by either varying the subjects sodium intake, water intake or inspired oxygen level [34, 35].

Due to the challenges associated with controlling subjects diet for two weeks as was performed in Priijm [36], the use of sodium intake was discounted. From previous work we know that applying a large water load to subjects during the scanning session, as in Tumkur and Prasad [37, 38], can cause undesired effects on the resultant shim, as assessed by B_0 maps, due to the large susceptibility change adding such a large quantity of water to the abdomen can cause, as such, this method was also discounted leaving us to pursue an oxygen challenge.

This method consisted of localisers and anatomical images being collected followed by alternating BOLD T_2^* and TRUST scans while the subject was breathing room air to record a baseline. Pure oxygen was then delivered to the subject at 15 ℓ/min via a gas mask and, after a two minute wash in period, the BOLD T_2^* and TRUST scans were repeated. A visual representation of this protocol can be seen in Figure 4.8. The BOLD T_2^* scans had a slice thickens of 5 mm, 12 echoes with an initial TE of 5 ms and subsequent echo spacing of 3 ms, the flip angle was 30°. The total scan time was approximately 17 seconds and was acquired during a single breath hold. The TRUST scans were conducted as per Section 4.2.2.

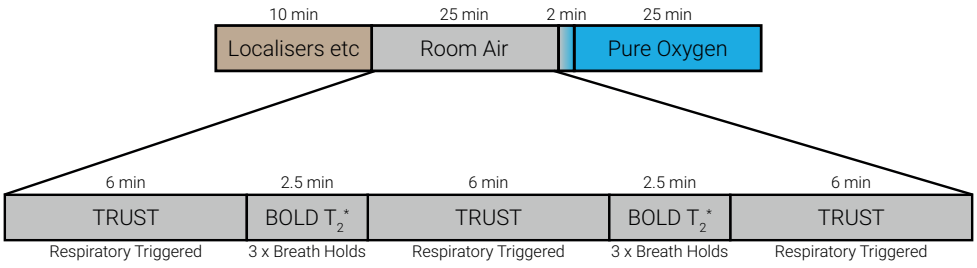

Figure 4.8: The protocol used to induce changes in renal oxygenation.

4.3 Results and Discussion

4.3.1 Susceptibility-Based Oximetry

Susceptibility-Based Oximetry in the Brain

Having collected data using the method outlined in 4.2.1 it was possible to use Equation (4.2) to estimate Y_v in the superior sagittal sinus to be $63 \pm 2.1\%$. This is consistent with the value reported by Liu of $61.1 \pm 1.4\%$ found in a multi centre TRUST trial with 250 participants over a wide range of ages and ethnicity distribution [15].

Susceptibility-Based Oximetry in the Renal Vein

Having calculated an acceptable result in the brain that agreed with literature it was possible to move onto applying techniques to assess oxygenation in the renal vein. A set of three phase maps were collected along with three localisers, one along each plane. If $\Delta\phi$ is plot against θ for a typical Y_v of 85%, Figure 4.9 is produced. It can be seen that, for an expected Y_v, the phase difference is greatest if the vessel runs parallel to the B_0 field. No part of the renal vein is located parallel to the B_0 field, typically the angle is in the region of 75° (there is a large degree of variability in vasculature geometry between subjects) and as such delivers a very small phase difference. This coupled with the fact that the gradient of this function at these angles is large, meaning that the uncertainty in angle corresponds to a larger uncertainty in Y_v means it will unfortunately not be possible to use SBO to accurately measure Y_v within the renal vein.

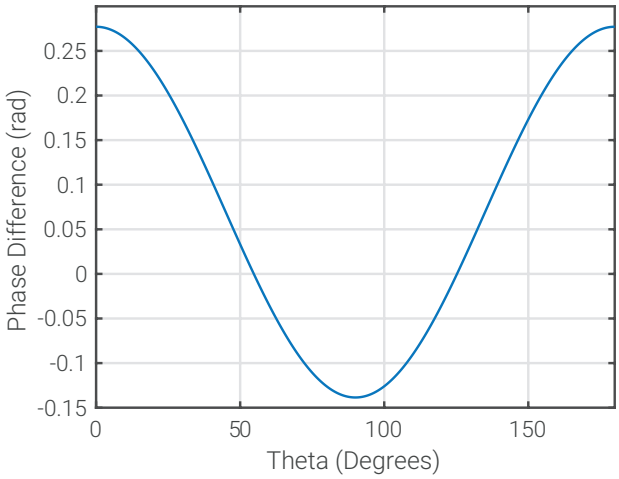

Figure 4.9: For a typical Y_v of 85% the phase difference produced by a vessel at a range of angles to B_0.

This technique would perhaps be better suited to use in the liver to assess oxygenation in the portal vein. This vessel runs at a much smaller angle to the B_0 field and as such the model will still be valid with reasonable errors, Figure 4.10. This would potentially work much better than TRUST here as the sequence is much quicker and therefore will be less susceptible to errors caused by movement.

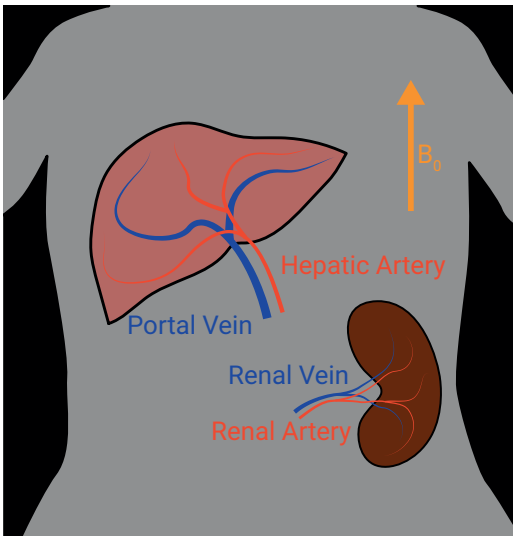

Figure 4.10: A schematic of the portal and renal veins entering the liver and left kidney respectively in relation to the B_0 field.

4.3.2 T_2 Relaxation Under Spin Tagging

TRUST in the Brain

To test if the FAIR labelling sequence delivered the same signal decay as the TILT sequence both labelling schemes were performed sequentially on the superior sagittal sinus with a PLD of 800 ms. The resulting normalised signals are shown in Figure 4.11.

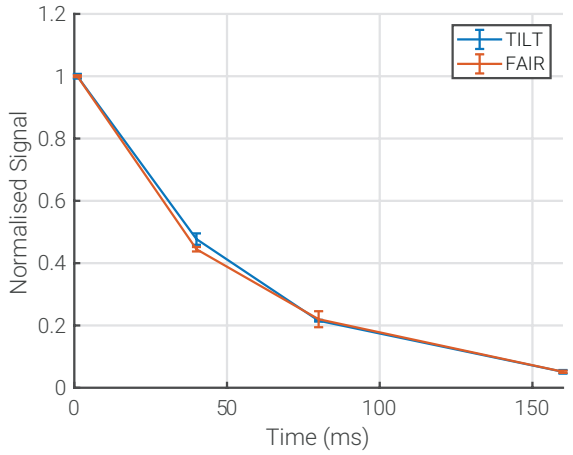

Figure 4.11: The signal decay within the superior sagittal sinus found using TRUST with both TILT and FAIR labelling sequences scaled by their initial signal intensities at eTE = 1 ms.

As can be seen these signals are in excellent agreement with the TILT sequence producing a T_2 of 52 ± 1 ms and the FAIR sequence producing a T_2 of 50 ± 2 ms, therefore in agreement within the bounds of error. This means that FAIR can be directly substituted for TILT in the TRUST sequence to measure Y_v in the superior sagittal sinus and can subsequently be used for the renal TRUST measurements.

To find the dependence PLD has upon the signal measured, scans were carried out at a range of delays from 400 ms to 1400 ms while using the FAIR labelling sequence. The signal from eTE=1 ms was then plot against label delay. Figure 4.12 shows the signal from the difference images. The maximum signal is observed with a PLD of 800 ms. This value is reached

due to the balance between T_1 relaxation of the non-selective blood and inflow of unlabelled blood. This maximum in signal agrees with literature using the TILT labelling scheme [12]. By carrying out scans with this PLD the maximum Signal to Noise Ratio (SNR) will be achieved.

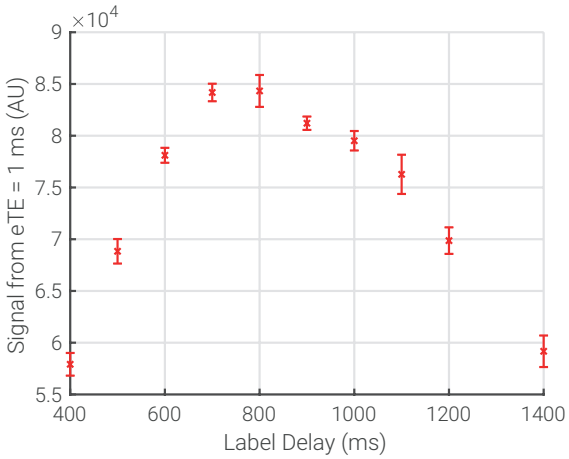

Figure 4.12: The mean signal from the first echo of each difference image over a range of PLD times.

T_2 should have no dependence upon PLD given the signal from the difference image will have the same decay in time, it will just be a lower intensity for non-optimal PLD thus leading to a larger confidence interval. To confirm this the fit values of T_2 were plot against PLD, Figure 4.13.

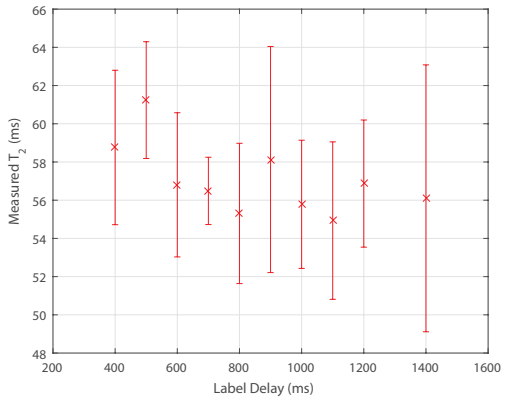

Figure 4.13: The dependence of T_2 upon PLD.

It can be seen that, as predicted, there is no relationship between T_2 and PLD. An increase in error with label delay was not observed, this effect may

only show itself at larger values of PLD however for our purposes, simply confirming there is no large increase in error around our chosen PLD is sufficient. This means that if there is a variation in the optimum PLD between subjects due to the larger range in RBF compared to Cerebral Blood Flow (CBF) then this will not have an affect upon the value of T_2 and thus Y_v.

When the analysis is carried out on the images, the four brightest voxels of the difference image are averaged before the fitting occurs. This number of voxels is chosen due to the average size of the superior sagittal sinus however, for some subjects more voxels could be included, potentially yielding better results. To assess the variability in T_2 measurements with the number of voxels averaged, the analysis was run multiple times with one to twelve voxels included in the calculation. Multiple TRUST scans were performed on the same subject and averaged generating Figure 4.14a.

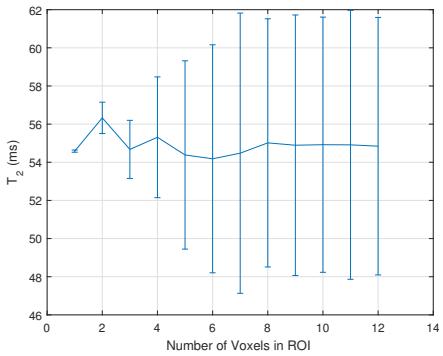

(a)

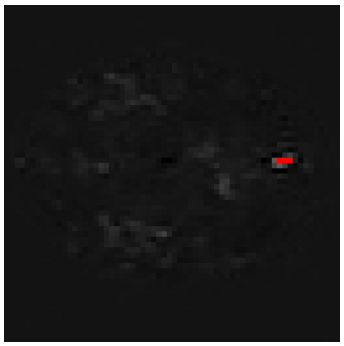

(b)

Figure 4.14: (a) The value of T_2 computed for the superior sagittal sinus with different numbers of voxels included in the calculation. (b) The difference image of the superior sagittal sinus with a three voxel ROI shown. This is already covering most of the vessel, hence the noise going up as more voxels are added to the calculation.

Although from Figure 4.14a it would appear that it would be best to only use the brightest voxel in the calculation due to its very small error and that it has the same value of T_2 as the results with far more voxels; this would not be a very robust method. It is fairly easy to conceive a greater than average level of

noise being recorded on a single voxel in the relaxation and as such skewing the output of the calculation. The confidence interval is so large above six voxels because by this point the calculations are simply including the noise around the vessel rather than the signal from the blood within the sagittal sinus. Given these results, using four voxels in the calculation seems to be a reasonable balance between uncertainty and robustness.

To assess the repeatability of this measure, the optimised scan was repeated ten times on a single subject during one scanning session. This yielded a Y_v of 69.5 ± 0.6%, a value consistent with literature [11, 15]. Given the success of the modified sequence on the superior sagittal sinus, it was possible to attempt to measure Y_v in the renal vein.

TRUST in the Body

Ideal vessels to test the TRUST sequence within the body are the portal vein and hepatic artery as these vessels are large, have different oxygen saturations and can easily be imaged at the same time. Using the modified TRUST sequence the T_2 and oxygen saturation of the portal vein was found to be 109 ± 5 ms and 79.9 ± 0.8 % respectively; the T_2 and oxygen saturation of the hepatic artery was found to be 157 ± 10 ms and 100 ± 1 % respectively. This means that, as expected, the oxygen saturation in the hepatic artery is measured as greater than that of the portal vein and therefore the TRUST protocol is working as expected. Although normally the analysis would simply be based upon the mean of the brightest voxels in the difference image as outlined in Section 4.2.2, in Figure 4.15 a voxel by voxel analysis has been carried out for illustrative purposes.

To assess if the PLD that generates the greatest signal is the same in the renal vein as in the superior sagittal sinus, a series of scans were collected with PLD ranging from 400 ms to 1400 ms and the signal from eTE = 1 ms recorded.

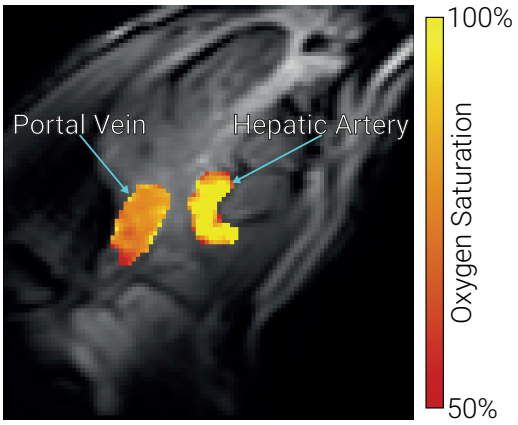

Figure 4.15: The oxygen saturation of the portal vein and hepatic artery measured using TRUST.

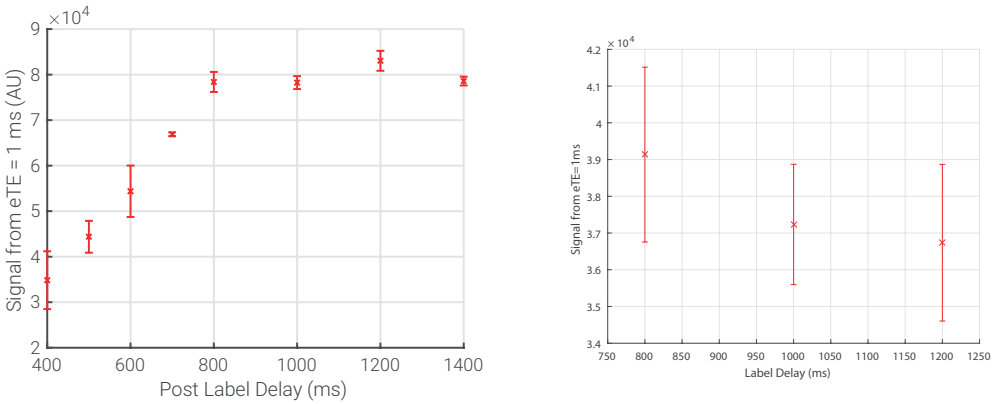

(a) (b)

Figure 4.16: (a) The mean signal from the first echo of each difference image of the renal vein over a range of PLD. (b) Mean signal from the first echo versus PLD from a different subject.

As seen in Figure 4.16a the PLD producing the largest signal in the difference image of the renal vein is indeed different to that of the superior sagittal sinus. This is most likely due to differences in blood flow through each of these vessels, 413 ± 136 ml/min in the renal vein [2] and 285 ± 19 ml/min in the superior sagittal sinus [7]. Given the much larger uncertainty in blood flow in the renal vein, a different subject was scanned over a smaller range of PLD to ascertain if the PLD delivering the maximum signal varies much between subjects, Figure 4.16b.

The maximum signal for the first subject was achieved at a PLD of 1200 ms whereas for the second subject the maximum is at a PLD of 800 ms. Given that these subjects had a RBF either side of the mean and that there is little dependence of T_2 upon PLD it seems appropriate to use a PLD of 1000 ms for optimum signal in most subjects.

Given the larger size of the renal vein compared to the superior sagittal sinus, it would be better to include more voxels in the calculations when fitting to find a value of T_2. Multiple scans were completed on a single subject and the value of T_2 found for each using one to twelve voxels in the fitting process. The results were averaged and plot in Figure 4.17a.

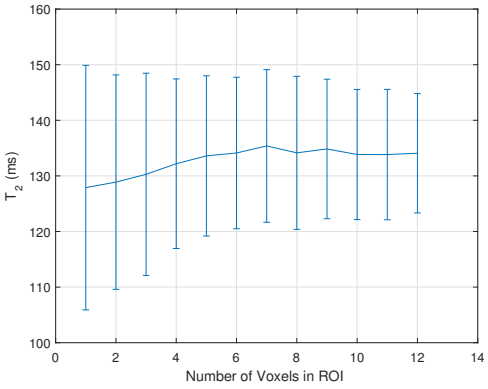

(a)

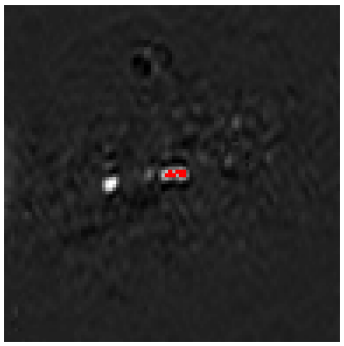

(b)

Figure 4.17: (a) The value of T_2 calculated for the renal vein with different numbers of voxels included in the calculation. (b) The difference image of the renal vein with a nine voxel ROI shown.

Unlike the results when this process was carried out on the superior sagittal sinus in Figure 4.14a, here the error decreases as more voxels are added to the calculation. This uncertainty comes from the large variation in T_2 for one voxel rather than a large error on the fit i.e. the error is coming from the differences between scans rather than the robustness of each scans results, this is precisely the concern that was raised with using a single voxel when discussing the superior sagittal sinus. As more voxels are added the error decreases until approximately six voxels are included, at this point the value of T_2 stops increasing and stays approximately constant. Once again, given

the large variation in renal veins, it would be advisable to include slightly more than six voxels but not so many that in the cases of small vessels the algorithm is sampling surrounding tissue. Nine voxels seems to be a suitable middle ground as to work effectively with both small and large vessels.

To assess the repeatability of the measurements within the kidney, the same scan was repeated ten times in a single session with the optimised renal parameters. This yielded a T_2 of 135 ± 5 ms corresponding to a Y_v of $89 \pm 2\%$. The variation in measurements of Y_v in the renal vein are relatively substantial and show no dependence upon time so are therefore not likely due to physiological changes. The value of Y_v in the renal vein is much higher than in the sagittal sinus however is within the range found by Nielsen [39].

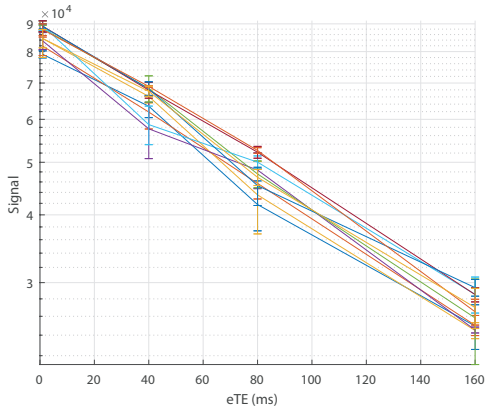

Figure 4.18: The T_2 relaxation curves of ten scans repeated on a single subject.

To compare the abilities of BOLD T_2^* maps and TRUST to measure changes in oxygenation in the kidneys, a hyperoxia challenge was conducted. In Figure 4.19a, no systematic, bulk change in T_2^* can be seen indicating that the change in T_2^* caused by the introduction of pure oxygen is dominated by other confounding factors. This is confirmed when ROI are defined for the renal cortex and renal medulla with the mean change in T_2^* found to be -2 ± 8 ms and -1 ± 6 ms respectively. When TRUST is used to measure the oxygen saturation in the renal vein an increase of 16 ± 3 % is observed, Figure 4.19b. This shows that it is possible to measure changes in renal oxygenation using TRUST that would be undetectable using the current standard, BOLD

T_2^* mapping.

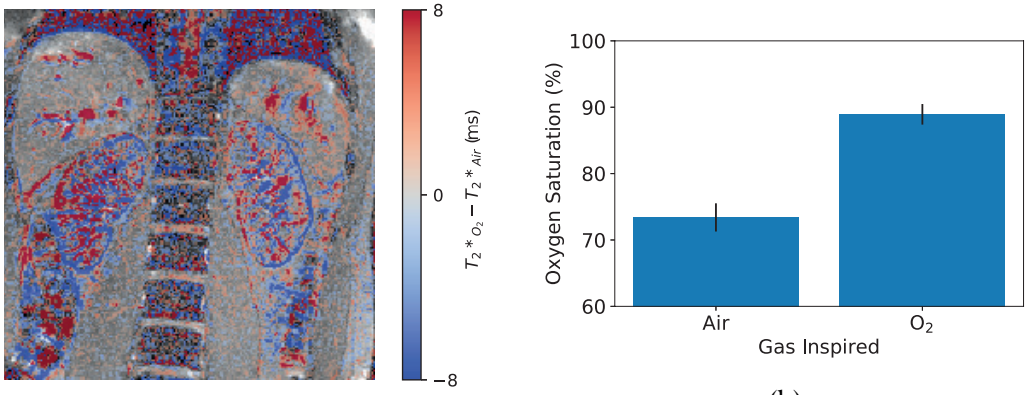

(a) (b)

Figure 4.19: (a), The difference in T_2^* measured between baseline and the hyperoxia state. (b) The difference in Y_v measured using TRUST.

4.4 Conclusions and Future Work

This work shows promising results for the use of a modified TRUST sequence to measure oxygenation of blood within the body. The existing TRUST sequence was modified to be respiratory triggered and use the FAIR labelling scheme making it suitable for use in the body. Once these modifications had been carried out, parameters such as PLD and the number of voxels used in the ROI were optimised. The ability of TRUST to measure a change in renal oxygenation was successfully verified via a hyperoxia challenge which was able to measure an increase of 16 ± 3 % where the current standard measurement of renal oxygenation, BOLD T_2^* maps, recorded no significant change.

Looking forward this work could be expanded by carrying out the hyperoxia challenge on more subjects. Although a small number of measurements were gathered on the hepatic vessels, further work could be undertaken to compare the use of SBO and TRUST to measure oxygenation in the portal vein in response to a hyperoxia challenge as conducted for the kidneys here. In the current protocol, haematocrit is assumed to be an average value of 0.41 unless a blood test has recently been undertaken. As stated above, there is a correlation between T_1 of blood and its haematocrit, this means that an estimate of the subjects haematocrit could be taken while they are in the scanner, thus leading to a more accurate measurement of oxygenation with only a small increase in scan time. This would be especially important when using TRUST on patients rather than healthy volunteers as their haematocrit has a larger variance.

4.5 Acknowledgements

We thank Hanzhang Lu for sharing the TRUST methodology.

4.6 References

1. Daniel, A., Cox, E., Buchanan, C., Bradley, C. & Francis, S. *Applying T2 Relaxation Under Spin Tagging (TRUST) to Assess Renal Oxygenation in the Kidney* in *Proc. Intl. Soc. Mag. Reson. Med. 26* International Society of Magnetic Resonance in Medicine Annual Meeting (Paris, 21st July 2018).
2. Cox, E. F. *et al.* Multiparametric Renal Magnetic Resonance Imaging: Validation, Interventions, and Alterations in Chronic Kidney Disease. *Frontiers in Physiology* **8.** ISSN: 1664-042X (2017).
3. Buchanan, C. E. *et al.* Quantitative Assessment of Renal Structural and Functional Changes in Chronic Kidney Disease Using Multi-Parametric Magnetic Resonance Imaging. *Nephrology Dialysis Transplantation* (29th June 2019).
4. Pruijm, M., Milani, B. & Burnier, M. Blood Oxygenation Level-Dependent MRI to Assess Renal Oxygenation in Renal Diseases: Progresses and Challenges. *Frontiers in Physiology* **7.** ISSN: 1664-042X. pmid: 28105019 (5th Jan. 2017).
5. Niendorf, T. *et al.* How Bold Is Blood Oxygenation Level-Dependent (BOLD) Magnetic Resonance Imaging of the Kidney? Opportunities, Challenges and Future Directions. *Acta Physiologica* **213,** 19–38. ISSN: 1748-1716.
6. Chong, S. P., Merkle, C. W., Leahy, C. & Srinivasan, V. J. Cerebral Metabolic Rate of Oxygen (CMRO2) Assessed by Combined Doppler and Spectroscopic OCT. *Biomedical Optics Express* **6,** 3941–3951. ISSN: 2156-7085 (11th Sept. 2015).
7. Jordan, J. E., Pelc, N. J. & Enzmann, D. R. Velocity and Flow Quantitation in the Superior Sagittal Sinus with Ungated and Cine (Gated) Phase-Contrast MR Imaging. *Journal of Magnetic Resonance Imaging* **4,** 25–28. ISSN: 1522-2586 (1st Jan. 1994).
8. Miao, G. *et al.* Reference Value of Presenile Human Hematocrit and Geographical Factors. *Journal of Clinical Laboratory Analysis* **16,** 26–29. ISSN: 1098-2825 (1st Jan. 2002).

9. Gardener, A. G., Francis, S. T., Prior, M., Peters, A. & Gowland, P. A. Dependence of Blood R2 Relaxivity on CPMG Echo-Spacing at 2.35 and 7 T. *Magnetic Resonance in Medicine* **64,** 967–974. ISSN: 1522-2594 (1st Oct. 2010).
10. Shimada, K., Nagasaka, T., Shidahara, M., Machida, Y. & Tamura, H. In Vivo Measurement of Longitudinal Relaxation Time of Human Blood by Inversion-Recovery Fast Gradient-Echo MR Imaging at 3T. *Magnetic resonance in medical sciences: MRMS: an official journal of Japan Society of Magnetic Resonance in Medicine* **11,** 265–271. ISSN: 1880-2206 (2012).
11. Nagdyman, N. *et al.* Comparison between Cerebral Tissue Oxygenation Index Measured by Near-Infrared Spectroscopy and Venous Jugular Bulb Saturation in Children. *Intensive Care Medicine* **31,** 846–850. ISSN: 0342-4642, 1432-1238 (1st June 2005).
12. Lu, H. & Ge, Y. Quantitative Evaluation of Oxygenation in Venous Vessels Using T2-Relaxation-Under-Spin-Tagging MRI. *Magnetic Resonance in Medicine* **60,** 357–363. ISSN: 1522-2594 (1st Aug. 2008).
13. Xu, F., Uh, J., Liu, P. & Lu, H. On Improving the Speed and Reliability of T2-Relaxation-Under-Spin-Tagging (TRUST) MRI. *Magnetic Resonance in Medicine* **68,** 198–204. ISSN: 0740-3194 (July 2012).
14. Liu, P., Xu, F. & Lu, H. Test–Retest Reproducibility of a Rapid Method to Measure Brain Oxygen Metabolism. *Magnetic Resonance in Medicine* **69,** 675–681. ISSN: 1522-2594 (1st Mar. 2013).
15. Liu, P. *et al.* Multi-Site Evaluations of a T2-Relaxation-Under-Spin-Tagging (TRUST) MRI Technique to Measure Brain Oxygenation. *Magnetic resonance in medicine* **75,** 680–687. ISSN: 0740-3194 (Feb. 2016).
16. Jain, V., Langham, M. C. & Wehrli, F. W. MRI Estimation of Global Brain Oxygen Consumption Rate. *Journal of Cerebral Blood Flow & Metabolism* **30,** 1598–1607. ISSN: 0271-678X (1st Sept. 2010).
17. Jain, V. *et al.* Cerebral Oxygen Metabolism in Neonates with Congenital Heart Disease Quantified by MRI and Optics. *Journal of Cerebral Blood Flow & Metabolism* **34,** 380–388. ISSN: 0271-678X (1st Mar. 2014).

18. Driver, I. D. *et al.* Global Intravascular and Local Hyperoxia Contrast Phase-Based Blood Oxygenation Measurements. *NeuroImage* **101,** 458–465. ISSN: 1053-8119 (1st Nov. 2014).

19. Lee, H., Langham, M. C., Rodriguez-Soto, A. E. & Wehrli, F. W. Multiplexed MRI Methods for Rapid Estimation of Global Cerebral Metabolic Rate of Oxygen Consumption. *NeuroImage* **149,** 393–403. ISSN: 1053-8119 (1st Apr. 2017).

20. Wright, G. A., Hu, B. S. & Macovski, A. Estimating Oxygen Saturation of Blood in Vivo with MR Imaging at 1.5 T. *Journal of Magnetic Resonance Imaging* **1,** 275–283. ISSN: 1522-2586 (1st May 1991).

21. Haacke, E. M. *et al.* In Vivo Measurement of Blood Oxygen Saturation Using Magnetic Resonance Imaging: A Direct Validation of the Blood Oxygen Level-Dependent Concept in Functional Brain Imaging. *Human Brain Mapping* **5,** 341–346. ISSN: 1097-0193 (1st Jan. 1997).

22. Spees, W. M., Yablonskiy, D. A., Oswood, M. C. & Ackerman, J. J. Water Proton MR Properties of Human Blood at 1.5 Tesla: Magnetic Susceptibility, T1, T2, T*2, and Non-Lorentzian Signal Behavior. *Magnetic Resonance in Medicine* **45,** 533–542. ISSN: 1522-2594 (1st Apr. 2001).

23. Jain, V., Abdulmalik, O., Propert, K. J. & Wehrli, F. W. Investigating the Magnetic Susceptibility Properties of Fresh Human Blood for Noninvasive Oxygen Saturation Quantification. *Magnetic Resonance in Medicine* **68,** 863–867. ISSN: 1522-2594 (1st Sept. 2012).

24. Jenkinson, M. Fast, Automated, N-Dimensional Phase-Unwrapping Algorithm. *Magnetic Resonance in Medicine* **49,** 193–197. ISSN: 1522-2594 (1st Jan. 2003).

25. Hendrikse, J., Lu, H., van der Grond, J., van Zijl, P. C. & Golay, X. Measurements of Cerebral Perfusion and Arterial Hemodynamics during Visual Stimulation Using TURBO-TILT. *Magnetic Resonance in Medicine* **50,** 429–433. ISSN: 1522-2594 (1st Aug. 2003).

26. Golay, X., Petersen, E. T. & Hui, F. Pulsed Star Labeling of Arterial Regions (PULSAR): A Robust Regional Perfusion Technique for High

Field Imaging. *Magnetic Resonance in Medicine* **53,** 15–21. ISSN: 1522-2594 (1st Jan. 2005).

27. Golay, X., Stuber, M., Pruessmann, K. P., Meier, D. & Boesiger, P. Transfer Insensitive Labeling Technique (TILT): Application to Multislice Functional Perfusion Imaging. *Journal of Magnetic Resonance Imaging* **9,** 454–461. ISSN: 1522-2586 (1st Mar. 1999).
28. Lu, H., Clingman, C., Golay, X. & van Zijl, P. C. Determining the Longitudinal Relaxation Time (T1) of Blood at 3.0 Tesla. *Magnetic Resonance in Medicine* **52,** 679–682. ISSN: 1522-2594 (1st Sept. 2004).
29. Silvennoinen, M., Clingman, C., Golay, X., Kauppinen, R. & van Zijl, P. Comparison of the Dependence of Blood R2 and R2* on Oxygen Saturation at 1.5 and 4.7 Tesla. *Magnetic Resonance in Medicine* **49,** 47–60. ISSN: 1522-2594 (1st Jan. 2003).
30. Liu, P. *et al.* T1 and T2 Values of Human Neonatal Blood at 3 Tesla: Dependence on Hematocrit, Oxygenation, and Temperature. *Magnetic Resonance in Medicine* **75,** 1730–1735. ISSN: 1522-2594 (Apr. 2016).
31. Lu, H. *et al.* Calibration and Validation of TRUST MRI for the Estimation of Cerebral Blood Oxygenation. *Magnetic Resonance in Medicine* **67,** 42–49. ISSN: 1522-2594 (1st Jan. 2012).
32. Martirosian, P., Klose, U., Mader, I. & Schick, F. FAIR True-FISP Perfusion Imaging of the Kidneys. *Magnetic Resonance in Medicine* **51,** 353–361. ISSN: 1522-2594 (1st Feb. 2004).
33. Liu, P., Cox, E. & Daniel, A. *Pro TRUST* version V2018.5. 23rd Aug. 2011.
34. O'Connor, J. P. *et al.* Comparison of Normal Tissue R1 and R*2 Modulation by Oxygen and Carbogen. *Magnetic Resonance in Medicine* **61,** 75–83. ISSN: 1522-2594 (1st Jan. 2009).
35. Donati, O. F., Nanz, D., Serra, A. L. & Boss, A. Quantitative BOLD Response of the Renal Medulla to Hyperoxic Challenge at 1.5 T and 3.0 T. *NMR in Biomedicine* **25,** 1133–1138. ISSN: 1099-1492 (1st Oct. 2012).

36. Pruijm, M. *et al.* Effect of Sodium Loading/Depletion on Renal Oxygenation in Young Normotensive and Hypertensive Men. *Hypertension* **55,** 1116–1122. ISSN: 0194-911X, 1524-4563 (1st May 2010).

37. Tumkur, S. M., Vu, A. T., Li, L. P., Pierchala, L. & Prasad, P. V. Evaluation of Intra-Renal Oxygenation during Water Diuresis: A Time-Resolved Study Using BOLD MRI. *Kidney International* **70,** 139–143. ISSN: 0085-2538 (1st July 2006).

38. Prasad, P. V. & Epstein, F. H. Changes in Renal Medullary pO2 during Water Diuresis as Evaluated by Blood Oxygenation Level–Dependent Magnetic Resonance Imaging: Effects of Aging and Cyclooxygenase Inhibition. *Kidney International* **55,** 294–298. ISSN: 0085-2538 (1st Jan. 1999).

39. Nielsen, K., Rehling, M. & Henriksen, J. H. Renal Vein Oxygen Saturation in Renal Artery Stenosis. *Clinical Physiology* **12,** 179–184. ISSN: 1365-2281 (1st Mar. 1992).